

## A kinetic study of nitrification inhibition in water distribution systems using low levels of chlorite

Mongkolaya Rungvetvuthivitaya, Rengao Song, Mark Campbell and Chittaranjan Ray

### ABSTRACT

Water utilities use operational strategies such as increasing pH, chlorine-ammonia ratio, and/or chloramine residual, distribution main flushing, and periodic break-point chlorination to control nitrification of chloraminated water in distribution systems. Although these methods are proven to be useful in controlling nitrification, the results are utility dependent and sometimes not effective in controlling the loss of chloramines. In various pilot studies, the direct application of chlorite at 0.1 to 0.8 mg/L is shown to be an effective alternative to control and prevent nitrification. Chlorite inactivates ammonia-oxidizing bacteria (AOB), the root cause of nitrification. In this study, we developed a kinetic model for nitrification inhibition through the addition of chlorite and the observation of residual chloramines and AOB. The important water quality variables examined were: chlorite concentration ranging from 0.02 to 0.4 mg/L, pH ranging from 7 to 9, ammonia concentrations ranging from 0.5 to 2.0 mg/L-N, and temperature ranging from 15 to 35 °C. Instead of measuring the viability of the AOB cells, the production of nitrite and the consumption of ammonia are used as surrogates for cell activity. This information was used to develop a kinetic model (modified Intrinsic Quenching model) that was able to fit the experimental data.

**Key words** | ammonia, chloramination of water, modified Intrinsic Quenching model, nitrification in drinking water, *Nitrosomonas europaea*, water distribution system

Mongkolaya Rungvetvuthivitaya  
Chittaranjan Ray (corresponding author)  
Department of Civil and Environmental  
Engineering and Water Resources Research  
Center,  
University of Hawaii,  
Honolulu, HI 96822,  
USA  
E-mail: [cray@hawaii.edu](mailto:cray@hawaii.edu)

Rengao Song  
Mark Campbell  
Louisville Water Company,  
Louisville, KY 40202,  
USA

### BACKGROUND

#### Chloramination and nitrification in distribution system

Chloramine is widely used as a secondary disinfectant to prevent microbial regrowth in water distribution systems. Numerous water utilities have switched their management strategies from using free chlorine to chloramine primarily because chloramination has been demonstrated to form less disinfection by-products (DBPs), such as trihalomethanes and haloacetic acids. The practice of chloramination is predicted to significantly increase for surface water treatment facilities (Yang *et al.* 2008).

Chloramine residual levels are found to decrease with the length of the distribution system. Several important water quality parameters affect the rate and mechanism of

chloramine decomposition. These parameters include pH, chlorine-ammonia ratio, temperature, characteristics of natural organic matter (NOM), as well as levels of total organic carbon and nitrite. In addition to the loss of chloramine due to its abiotic decomposition, nitrification of ammonia can reduce chloramine levels dramatically. The frequency and degree of nitrification are more pronounced during high-temperature summer seasons. A survey of utilities that use chloramines indicated that 63% have experienced nitrification episodes (Wilczak *et al.* 1996).

As outlined in the Total Coliform Rule (United States Environmental Protection Agency (USEPA) 1989), the loss of disinfectant residual could pose a health risk to the public. As per the Surface Water Treatment Rule (SWTR;

see USEPA 1989), 95% of samples from a distribution system must have a disinfectant residual greater than 0.2 mg/L of chlorine. In addition, nitrification increases the levels of nitrite and nitrate, which are regulated contaminants. The maximum contaminant levels (MCL) of nitrite and nitrate are 1 and 10 mg/L-N, respectively (USEPA 2009).

Operational strategies that have been used to control nitrification include raising the pH of the water, reducing the age of water, increasing the chlorine-ammonia ratio, increasing chloramine residual concentration, distribution main flushing, periodic break-point chlorination, and NOM removal (Odell *et al.* 1996; Harrington *et al.* 2002; Skadsen 2002). While some of these operational practices have been successful, it appears that the outcomes are utility dependent. Moreover, some of these strategies can pose significant operational and/or financial difficulties.

### Health risk of direct application of low levels of chlorite

One major barrier to directly applying chlorite as a nitrification inhibitor is the fact that chlorite is a regulated chemical with an MCL of 1.0 mg/L and a maximum contaminant level goal (MCLG) of 0.8 mg/L (USEPA 2009). The concentration of chlorite used in this study was less than 0.4 mg/L, or less than 50% of the MCLG.

In 2002, the Agency for Toxic Substances and Disease Registry (ATSDR) issued a draft for the Toxicological Profile of Chlorine Dioxide and Chlorite (ATSDR 2004). The report gave a minimal risk level of 0.1 mg/kg/day intermediate-duration oral exposure (15–364 days) for chlorite. The USEPA has derived a reference dose (RfD) of 0.03 mg/kg/day for chlorite. Considering an adult body weight of 70 kg and a water consumption rate of 2 L/day, the RfD of chlorite would be 1.05 mg/L (or  $(0.03 \text{ mg/kg/day} \times 70 \text{ kg})/2 \text{ L/day}$ ). The levels of chlorite in this study are below 0.4 mg/L, or 38% of the suggested RfD.

### Nitrification inhibition by chlorite

One of the earliest works on the inhibition of chemoautotrophic nitrification by chlorite was conducted by Hynes & Knowles (1983) to prevent loss of ammonium fertilizer due to nitrification. They conducted their experiments in a soil environment that had a high ammonia concentration

of 2 mM (28 mg/L-N) and a cell concentration of  $960 \times 10^6$  cells of ammonia oxidizing bacteria (AOB)/mL.

The use of chlorite to inhibit nitrification in drinking water was first investigated by McGuire *et al.* (1999). Their experiments lasted for 24 h and the concentration of AOB was monitored using a most-probable-number (MPN) technique. Chlorite at concentrations of 0.05, 0.2, and 1.0 mg/L was applied to the bench-scale experiments with varying concentrations of AOB (190–91,000 MPN/mL). At the end of the experiments, counts of AOB were less than the detection limit of 0.2 MPN/mL. The effect of chlorite on the heterotrophic plate count (HPC) and *Escherichia coli* bacteria was also evaluated with chlorite dosages of 0.1, 0.3, and 1.0 mg/L. The results showed that HPC and *E. coli* numbers were affected by chlorite at all tested concentrations. Field investigation at their facility also confirmed that the presence of chlorite could retard nitrification. Utilities that have chlorite present in the distribution systems lose less chloramine and ammonia-nitrogen than those without chlorite.

A full-scale experimental verification was undertaken at the Willmar (Minnesota) Municipal Utilities (O'Connor *et al.* 2001) by adding sodium chlorite directly into the finished water leaving the treatment plant. Three weeks after the initial feed, nitrification in the distribution system was significantly decreased. Oxygen and chloramine residuals at sampling sites increased after the application of chlorite. There was no information available regarding the chlorite levels and the duration of application.

Two additional studies have been reported for pilot-scale nitrification inhibition. The first study was conducted in a pipe-loop apparatus (Passantino *et al.* 2003). It consisted of two connected loops that represented a transmission line and distribution line with sections of pipes taken from a distribution system. The feed water consisted of the finished water from the Union Hills Water Treatment Plant, Phoenix, AZ with a chlorine residual of 3.0 mg/L-Cl<sub>2</sub> and Cl<sub>2</sub>:NH<sub>3</sub>-N ratio of 3:1. Chlorite was fed at 0.5 mg/L, but it decayed in the system to less than 0.1 mg/L after a retention time of about 5 days. There were two explanations for the decay: (1) chlorite could have combined with free chlorine due to mixing issues, or (2) chlorite was biologically reduced to chloride. McGuire *et al.* (2006) conducted another study using pilot bioreactors. The control treatment units were

fed with chloramines at 1.5 mg/L-Cl<sub>2</sub> with a Cl<sub>2</sub>:NH<sub>3</sub>-N ratio of 3:1. Other units were tested for the effect of chlorite concentration and feed method. The chlorite feed method was tested in two ways: continuous or intermittent feed (for 1 week). For the continuous feed method, chlorite was dosed at 0.1, 0.2, 0.4, and 0.8 mg/L for approximately 17 weeks for each concentration. The results indicated that none of the units showed any development of nitrification. For intermittent dosages, units that received chlorite at 0.2 mg/L for 1 week stopped nitrification for 3 to 4 weeks; then nitrification began to reestablish itself. *McGuire et al. (2009)* fed sodium chlorite to an isolated area of the water distribution system of the city of Glendale, CA. They showed that nitrification was prevented in reservoirs for several months. *Blute et al. (2013)* conducted a chlorite feed study on a reservoir of the water distribution system of Irvine Ranch Water District in Irvine, CA. The reservoir had two identical cells. One cell received chlorite at 0.3 and 0.6 mg/L and the other was used as control (no chlorite). They observed severe nitrification in the control cell over the next 6 months and none was observed in the treated cells.

Based on the current status of research relating to nitrification inhibition using chlorite, the objective of this study was to provide an in-depth understanding of the inhibition kinetics in the presence of chlorite through mathematical modeling. Bench-scale experiments were conducted in order to obtain the kinetic model parameters.

## MATERIALS AND METHODS

### Materials and preparation methods

Sodium chlorite used in the experiment was obtained from the JT Baker Company (now part of Avantor Performance Materials), Center Valley, PA. The purity was 79%. A stock solution of sodium chlorite was prepared with a concentration of 1,000 mg/L. An ammonia stock solution at a concentration of 1,000 mg/L-N was prepared from ammonium sulfate (NH<sub>4</sub>)<sub>2</sub>SO<sub>4</sub> (purchased from VWR Scientific).

A culture of the bacterium *Nitrosomonas europaea* ATCC 25978 was obtained from the American Type Culture

Collection (ATCC, Rockville, MD). The culture was grown in ATCC medium 2265 in 250 mL-Erlenmeyer flasks on a water bath rotary shaker (100 rpm) at 30 °C in the dark. Three different media were made composed of the following ingredients: Medium 1: (NH<sub>4</sub>)<sub>2</sub>SO<sub>4</sub>, 4.95 g; KH<sub>2</sub>PO<sub>4</sub>, 0.62 g; MgSO<sub>4</sub> (1.0 M stock solution), 1.1 mL; CaCl<sub>2</sub> (1.0 M stock solution), 0.3 mL; FeSO<sub>4</sub> (30 mM in 50 mM ethylenediamine tetra-acetic acid [EDTA] at pH 7), 0.5 mL; CuSO<sub>4</sub> (50 mM stock solution), 0.02 mL; distilled water, 1.2 L. Medium 2: KH<sub>2</sub>PO<sub>4</sub>, 8.2 g; NaH<sub>2</sub>PO<sub>4</sub>, 0.7 g; distilled water 300 mL; and bring the pH to 8 with 10 N NaOH. Medium 3 (buffer): 5% (w/v) Na<sub>2</sub>CO<sub>3</sub> anhydrous, 12 mL. The three media were autoclaved separately and then combined when cooled to room temperature. The culture was checked for contamination by spreading 100 µL of culture on a Luria Bertani agar plate and incubating it overnight (or 24 h) at 37 °C.

Cells were harvested during the late exponential growth phase (3–4 days after inoculation) by centrifugation (10,000 × *g* for 10 min). During this period the cells are expected to be in a state of high activity. The term ‘activity’ of the cell is defined as having the ability to consume ammonia and to produce nitrite. The cells were resuspended and centrifuged three times in sodium phosphate buffer (50 mM NaH<sub>2</sub>PO<sub>4</sub>, 2 mM MgCl<sub>2</sub>, pH 8). The concentration of the cells was quantified by the BacLight technique (Molecular Probes, Inc., Eugene, OR; *Boulos et al. 1999*).

### Analytical methods

Chlorite and nitrate were analyzed by ion chromatography using EPA Method 300.1 (*USEPA 1997*). Nitrite and ammonia were measured using a HACH spectrophotometer DR4000. The methods used for nitrite and ammonia measurement were Diazotization Method 10019 and Salicylate Method 10023, respectively (HACH Company, Loveland, CO).

Cell concentration of AOB was quantified before inoculation using LIVE/DEAD BacLight Bacterial Viability Kits (Catalog Number – L-7012, Molecular Probes, Inc., Eugene, OR; which is part of Life Technologies of Thermo Fisher). The concentration procedure directly followed that outlined in *Oldenburg et al. (2002)*. Briefly, the staining solution was added to the cells previously concentrated on

0.2 µm blackened polycarbonate filters (Osmonics, Minnetonka, MN) and incubated in the dark at room temperature for 15 min. The cells were visualized through a Zeiss Axioscope microscope (Carl Zeiss MicroImaging, Inc., Thornwood, NY) and images were captured with a video camera (Optronics DEI-750, Optronics, Goleta, CA) at 1,000× magnification. As outlined in Oldenburg *et al.*, we captured two images for each field using two filter sets (#CZ 910 and #CZ 915, Chroma Technology, Brattleboro, VT) for the green (viable cells) and red (nonviable cells) fluorescing bacteria. The two images were then combined to count the cells showing green and red using Adobe Photoshop (San Jose, CA). For each sample, 15 fields were randomly selected and the cells were counted. Cell concentration can be calculated according to Equation (1)

$$N = \left( \frac{\bar{N}_{\text{image}}}{A_{\text{image}}} \right) \left( \frac{A_{\text{filter}}}{V_{\text{sample}}} \right) \quad (1)$$

where  $N$  is cell concentration (cells/mL),  $\bar{N}_{\text{image}}$  is the average number of cells per image,  $A_{\text{image}}$  and  $A_{\text{filter}}$  are the areas of filter captured in each image (0.013 mm<sup>2</sup>) and the total filtration area (415.48 mm<sup>2</sup>), respectively, and  $V_{\text{sample}}$  is the sample volume (mL).

Once the experiment started, cells were collected at days 0, 2, and 5 and quantified by using both the BacLight technique (Molecular Probes, Inc., Eugene, OR) and real-time polymerase chain reaction (PCR). The real-time PCR followed the protocol presented by Harms *et al.* (2003). The primers used targeted the AOB 16S rDNA gene. The samples were analyzed by a contract laboratory at the Biotechnology Center, Western Kentucky University, Bowling Green, KY.

### Experimental matrix design

A kinetic inhibition model was developed after collecting experimental batch kinetic data for the effects of chlorite, including nitrite production and ammonia consumption. Table 1 presents the AOB inhibition experimental sets. As can be observed from this table, chlorite concentrations varied between 0.02 and 0.4 mg/L, ammonia between 0.5 and 2.0 mg/L, temperature between 15 and 35 °C, and pH between 7 and 9.

**Table 1** | Experimental variables of orthogonal matrix

Set	pH	Chlorite (mg/L)	Initial NH <sub>3</sub> (mg/L)	No. of cells (1,000 × cells/mL)	Temperature (°C)
1	7	0, 0.02, 0.05, 0.1, 0.4	1.0	400	30
2	8	0, 0.02, 0.05, 0.1, 0.4	1.0	400	30
3	9	0, 0.02, 0.05, 0.1, 0.4	1.0	400	30
4	8	0, 0.02, 0.05, 0.1, 0.4	0.5	400	30
5	8	0, 0.02, 0.05, 0.1, 0.4	2.0	400	30
6	8	0, 0.02, 0.05, 0.1, 0.4	1.0	400	15
7	8	0, 0.02, 0.05, 0.1, 0.4	1.0	400	22
8	8	0, 0.02, 0.05, 0.1, 0.4	1.0	400	35

Bench-scale experiments were conducted using sterile 1,000 mL amber bottles serving as batch reactors. Buffered water was prepared from sodium phosphate, monobasic (NaH<sub>2</sub>PO<sub>4</sub>) and/or sodium phosphate, and dibasic (Na<sub>2</sub>PHO<sub>4</sub>) at 10 mM using reverse osmosis water. The pH was adjusted to the target value by the addition of either NaOH or HCl. These solutions were autoclaved before adding the cells. Once the solutions cooled, the cell suspensions were added to obtain the target concentration, and spiked with various concentrations of chlorite. The bottles were incubated at specific temperatures (see Table 1) in an oven or refrigerator. Each experiment had a control in which there was no addition of chlorite. These inhibition experiments were carried out in duplicate.

### Modified intrinsic quenching (IQ) model development

Several models such as Chick–Watson and Hom (Hom 1972; Chick 1908; Watson 1908) have been used to describe the inactivation of microorganisms by chemical disinfectants. These models are frequently used to simulate the inactivation kinetics of microorganisms such as *Nitrosomonas europaea*, *Cryptosporidium parvum*, and *Giardia lamblia* in drinking water (Finch *et al.* 1993a, b; Oldenburg *et al.* 2002). These chemical disinfection models are used to describe the ratio of surviving microorganisms to those inactivated by disinfectants with time.

The AOB (MPN method, see Wolfe *et al.* 1990; bacterial viability test, and real-time PCR) procedures for enumeration are time-consuming, costly, and less accurate

compared to measuring nitrite and ammonia concentrations. Therefore, in this study, modeling was used to estimate the ratio of the cell activity that was inhibited by chlorite with time. This study introduces a new perspective on the use of models and describes the inhibition through the use of disinfection kinetic modeling. When plotting the natural log of the ammonia concentration-time curve, if the graphs display a high degree of tailing, they cannot be modeled by either the Chick–Watson or the Hom models. Lambert & Johnston (2000) introduced the IQ model for log-survivor versus time data, which shows a long degree of tailing (see Table 2, left panel). In the Lambert and Johnston IQ model, the curve with the highest disinfectant concentration indicates the greatest inactivation and is the top-most in the series of curves (see Lambert & Johnston (2000) for details). Our studies show that the inhibition curve with the highest chlorite concentration shows the most inhibition will be at the bottom-most in the series of curves. Since ammonia concentration and the number of live cells are inversely related, the IQ model should be modified.

We modified the IQ model by inverting the chlorite concentration ( $1/C_0$ ) and introducing a coefficient  $n^*$  to the equation. The rate constants  $k_1$  (rate of AOB activity) and  $k_2$  (rate of chlorite effectiveness) are described in Figure 1. In this figure, the activity of an inoculum of *N. europaea* is inhibited by the presence of chlorite. The activity of the cells (less/no consumption of ammonia and less/no production of nitrite) is a rate governed by  $k_1$ . At the same

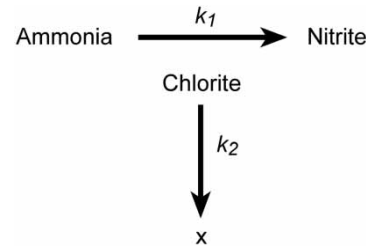


**Figure 1** | Basis for the modified IQ model of *N. europaea* and chlorite inactivation (modified after Lambert & Johnston 2000).

time, the chlorite effectiveness lessens (has less/no effect on the cells) at a rate governed by  $k_2$ .

As inhibition occurs over time, the activity of the AOB was measured and their activity decreased as chlorite concentration increased. For general use of the disinfection equation, the number of dead organisms increases as the disinfectant concentration increases. Therefore, the following equation used in our work is termed a modified IQ model (mIQ)

$$\ln(A_0/A) = \frac{k_1(1/C_0)^{n^*}}{Q}(1 - e^{-Qt}) \quad (2)$$

where  $A_0/A$  = ratio of initial  $\text{NH}_3$  and  $\text{NH}_3$  (at time  $t$ ) concentration,  $k_1$  = rate of AOB activity (per h),  $n^*$  = dilution coefficient,  $Q = k_2 \times n^*$ , amount of curvature;  $k_2$  is rate of chlorite effectiveness (per h),  $t$  = time (h),  $C_0$  = initial chlorite concentration (mg/L).

Table 2 shows the difference in the equation format and the meaning of parameters between the traditional IQ model and mIQ model. The input ammonia concentration to Equation (2) is within the detection limit of ammonia and not equal to zero.

**Table 2** | Parameter definition of IQ model and modified IQ model

IQ model		Modified IQ model	
$\ln(N_0/N) = \frac{k_1 C_0^n}{Q}(1 - e^{-Qt})$		$\ln(A_0/A) = \frac{k_1(1/C_0)^{n^*}}{Q}(1 - e^{-Qt})$	
$N$	number of surviving microbes	$A$	concentration of ammonia (AOB activity)
$C_0$	initial biocide concentration	$(1/C_0)$	reciprocal initial chlorite concentration
$n$	dilution coefficient	$n^*$	dilution coefficient
$k_1$	rate of microbes become nonviable	$k_1$	rate of AOB activity
$k_2$	rate of biocide inactivation	$k_2$	rate of chlorite effectiveness

Note:  $Q = k_2 \times n$ , or  $k_2 \times n^*$ ;  $N_0$  and  $A_0$  imply starting values.

## RESULTS AND DISCUSSION

In the inhibition experiments, nitrite production was used as a proxy for cell activity since the added ammonia was metabolized by *N. europaea* used in the batch experiments. Nitrite is a product of the activity of *N. europaea* (Hooper 1989). The initial conversion of ammonia to nitrite is problematic because nitrite in water will react chemically with chloramines leading to the reduction of disinfectant

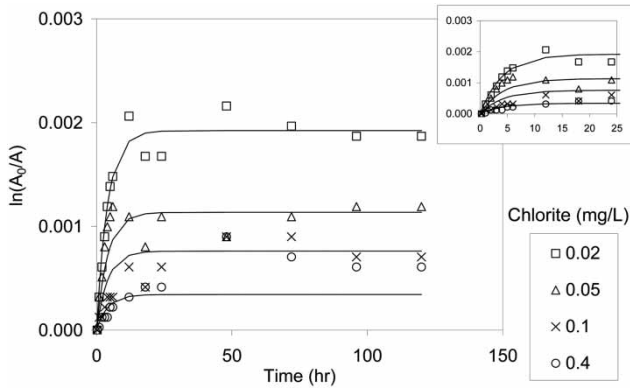


**Figure 2** | Inhibition kinetics of chlorite (mg/L). Set 1: pH 7,  $\text{NH}_3 = 1.0$  mg/L-N,  $30^\circ\text{C}$  temperature. Note: observed = symbols and modeled = lines.

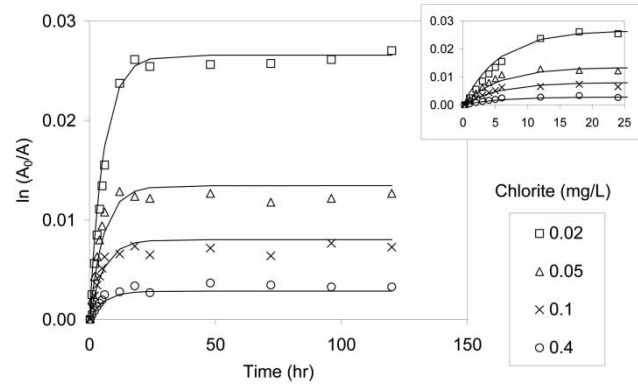


**Figure 3** | Inhibition kinetics of chlorite (mg/L). Set 2: pH 8,  $\text{NH}_3 = 1.0$  mg/L-N,  $30^\circ\text{C}$  temperature (baseline condition). Note: observed = symbols and modeled = lines.

residual. The decomposition of chloramines releases ammonia which serves as a food source for AOB. This further enhances the degree of nitrification. Episodes of nitrification in full-scale distribution systems are normally detected by an increase in the level of nitrite (Odell *et al.* 1996; Wilczak *et al.* 1996; McGuire *et al.* 1999, 2009; Skadsen 2002). The procedure for measuring nitrite concentration is not only simpler, but less time consuming, less expensive, and more accurate than enumerating AOB, making it easier for water utilities to measure nitrite on a routine basis.

Based on our experimental design presented in Table 1, there were a total of eight sets of experiments in which pH, initial ammonia concentration, and temperature were varied. Each set generated four curves representing chlorite concentrations of 0.02, 0.05, 0.1, and 0.4 mg/L. Set two served as a base-case condition. In this case, pH was set at 8, ammonia concentration at 1 mg/L-N, and incubation temperature at  $30^\circ\text{C}$  (Figure 3). The chlorite concentration remained unchanged throughout the incubation period. For each set, the coefficient  $k_1$  (rate of inhibition),  $n^*$  (dilution coefficient), and  $Q$  (amount of curvature) were obtained by fitting these parameters using a statistical program (Igor, WaveMetrics, Inc., Lake Oswego, OR). The experimental data and the fitted curves are displayed in Figures 2–9. The fitted parameters for these results are shown in Table 3.

As expected, the higher the chlorite concentration, the lower the ammonia consumption was in every set. As chlorite continued to be in contact with *N. europaea*, the activity

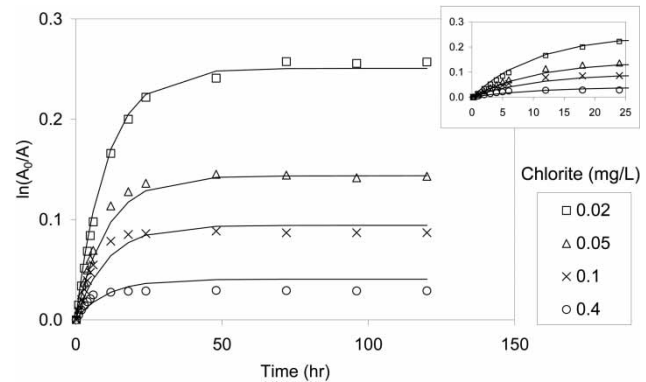


**Figure 4** | Inhibition kinetics of chlorite (mg/L). Set 3: pH 9,  $\text{NH}_3 = 1.0$  mg/L-N,  $30^\circ\text{C}$  temperature. Note: observed = symbols and modeled = lines.

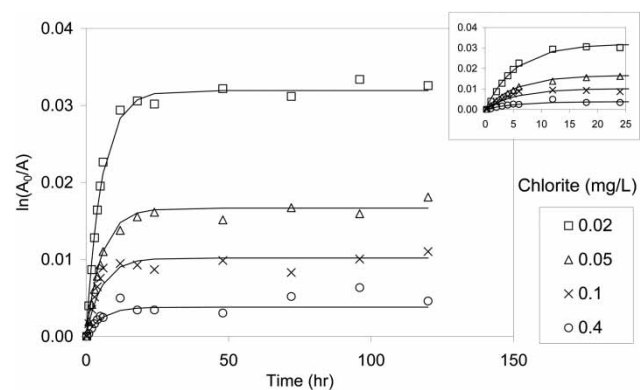


**Figure 5** | Inhibition kinetics of chlorite (mg/L). Set 4: pH 8,  $\text{NH}_3 = 0.5$  mg/L-N,  $30^\circ\text{C}$  temperature. Note: observed = symbols and modeled = lines.

of the bacteria became less as time progressed until no activity was observed. The time required for complete inhibition of *N. europaea* activity depended on chlorite dosage and contact time. The concentration  $\times$  time (CT) concept

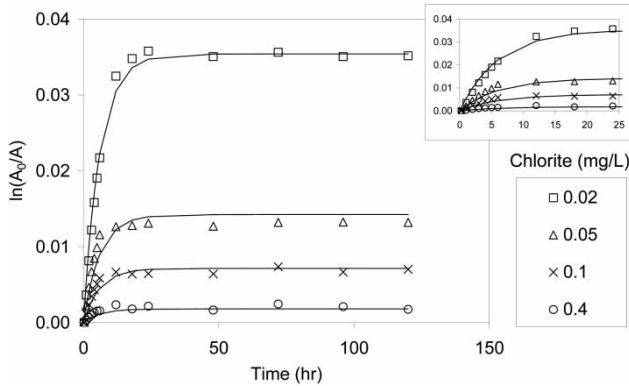


**Figure 6** | Inhibition kinetics of chlorite (mg/L). Set 5: pH 8,  $\text{NH}_3 = 2.0$  mg/L-N, 30 °C temperature. Note: observed = symbols and modeled = lines.

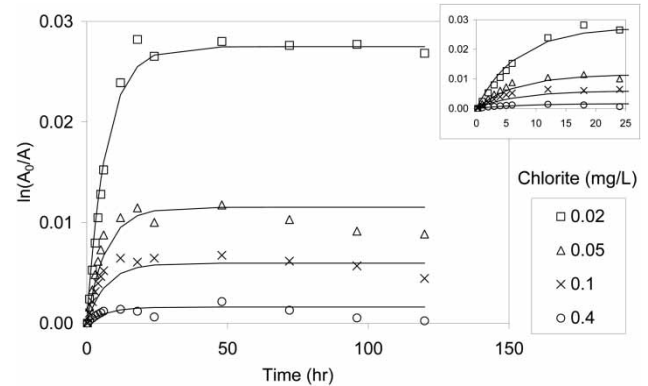


**Figure 8** | Inhibition kinetics of chlorite (mg/L). Set 7: pH 8,  $\text{NH}_3 = 1.0$  mg/L-N, 22 °C temperature. Note: observed = symbols and modeled = lines.

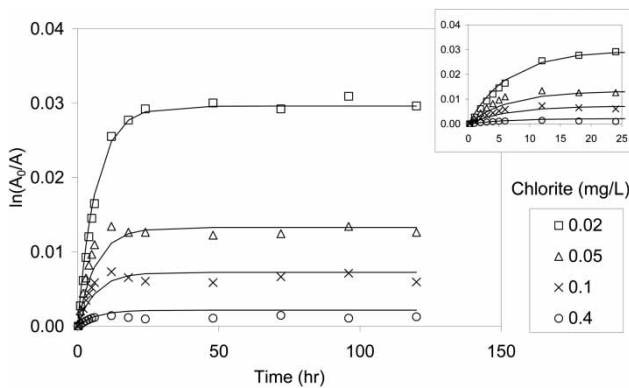


**Figure 7** | Inhibition kinetics of chlorite (mg/L). Set 6: pH 8,  $\text{NH}_3 = 1.0$  mg/L-N, 15 °C temperature. Note: observed = symbols and modeled = lines.

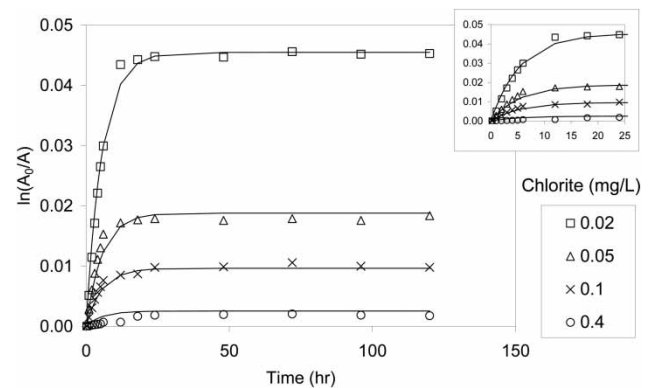


**Figure 9** | Inhibition kinetics of chlorite (mg/L). Set 8: pH 8,  $\text{NH}_3 = 1.0$  mg/L-N, 35 °C temperature. Note: observed = symbols and modeled = lines.

was applied to explain the chlorite dose and contact time required to inhibit the *N. europaea* activity (Rungvetvuthitaya et al. 2008).

Figures 2–4 show that the pH varied as 7, 8, and 9, respectively. Other parameters such as initial ammonia concentration and incubation temperature were the same. Significant inhibition (1-log or 90%) was observed between different pH sets. Figures 2–4 show that *N. europaea* appeared to be more resistant to chlorite at higher pH levels. Figures 3, 5, and 6 had initial ammonia concentrations of 1.0, 0.5, and 2.0 mg/L, respectively. These graphs do not indicate a significant degree of AOB inhibition at any of the three concentrations (less than 1-log difference among each set). The same observation is true for Figures 3 and 7–9 in which the temperature varied from 15 to 35 °C.

Modeling results (Figures 2–9) show that chlorite at concentrations as low as 0.02 mg/L appeared to inhibit the

production of nitrite and consumption of ammonia within 72 h. The chlorite concentration of 0.4 mg/L appeared to stop the production of nitrite and consumption of ammonia within 24 h of application. These results indicate that chlorite has the ability to inhibit the activity of *N. europaea*. The flat portion of the curves confirms that chlorite has the ability to suppress *N. europaea*'s activity for at least 5 days within the detention time for most water distribution systems.

The modeled and the observed data were statistically compared using the average of the residuals (difference between the predicted and observed values) and standard deviation of the residuals. Table 3 presents the result of the fitted coefficient values with precision ( $\pm$ ) and residuals (mean value of the residuals and standard deviation of the residuals) of each set of experimental conditions.

**Table 3** | Modified IQ model parameters

Experimental condition <sup>a</sup>	$k_1 \times 10^{-5}$	Precision ( $\pm$ ) $\times 10^{-5}$	$n^*$	Precision ( $\pm$ )	Q	Precision ( $\pm$ )	Mean $\times 10^{-5b}$	S.D. $\times 10^{-5c}$
Set 1 (pH 7)	5	0.9	0.58	0.043	0.24	0.030	-0.6	19
Set 2 (pH 8, NH <sub>3</sub> = 1.0 mg/L, 30 °C)	26	2.0	0.74	0.019	0.18	0.008	0.9	93
Set 3 (pH 9)	219	13.8	0.61	0.015	0.09	0.004	-8.2	752
Set 4 (NH <sub>3</sub> = 0.5 mg/L)	36	2.4	0.71	0.016	0.18	0.007	-2.4	98
Set 5 (NH <sub>3</sub> = 2.0 mg/L)	12	1.0	0.99	0.021	0.17	0.006	3.5	96
Set 6 (15 °C)	15	1.5	0.87	0.025	0.15	0.008	-5.4	111
Set 7 (22 °C)	10	1.2	0.95	0.030	0.15	0.008	-0.2	111
Set 8 (35 °C)	19	1.3	0.96	0.018	0.18	0.006	-18.4	108

Note: Value of residual = observed  $\ln(A_0/A)$  - calculated  $\ln(A_0/A)$ .

<sup>a</sup>Refer to Table 1.

<sup>b</sup>Mean = mean value of residuals.

<sup>c</sup>S.D. = standard deviation of residuals.

The coefficients  $k_1$ ,  $n^*$ , and Q range from  $4.93 \times 10^{-5}$  to  $2.19 \times 10^{-3}$  per hour, 0.58 to 0.99 (dimensionless), and 0.09 to 0.24 per hour, respectively. The precisions are all less than one significant digit of the predicted value. Each coefficient was plotted for comparison (Figures S-1–S-3, available online at <http://www.iwaponline.com/jws/063/135.pdf>). It was observed that the  $k_1$  values of experiment Set 1 had the lowest value and Set 3 had the highest value (Figure S-1). The rest of the data sets had  $k_1$  values in a close range. To verify this observation statistically, a graph of the  $k_1$  value was plotted for comparison along with the value from the normal distribution curve 95% and 99% confidence interval by accounting for only Sets 2, and 4–8 that were all conducted at pH 8 (Figure S-1). Similar plots were prepared for both coefficients  $n^*$  and Q (Figures S-2 and S-3). Based on the 99% confidence interval in these three plots, coefficients  $k_1$  and Q appear to be dependent on pH. On the other hand, coefficient  $n^*$  appears to be independent of pH at levels from 7–9. The plots also suggest that initial ammonia concentration (Sets 2, 4, and 5) and temperature (Sets 2 and 6–8) have less effect on  $k_1$ ,  $n^*$ , and Q values based on the 99% confidence interval. In other research, the value of  $n$  has been shown to be independent of temperature (20–35 °C) for phenol and *E. coli* (Hugo & Denyer 1987).

Coefficient  $k_1$  and pH values can be related by an exponential fit based on the three experimental data points shown in Figure S-1. The equation is given by

$$k_1 = 8 \times 10^{-11} e^{1.897 \text{ pH}} \quad (3)$$

The plot indicates that coefficient  $k_1$  increases rapidly between pH ranging from 8 to 9 compared to pH ranging from 7 to 8. When the pH value increases, the AOB appear to be more resistant to the exposure of chlorite that leads to a higher rate of AOB activity. This confirms the findings of a previous study (Oldenburg et al. 2002) where an increase in pH lowered the rate of inactivation of *N. europaea* by chloramine.

For all experiments, the  $n^*$  values lie within the 99% confidence interval, with an average of 0.80. As expected, the  $n^*$  values were less than 2 which suggests that the mechanism of chlorites inhibition of *N. europaea* may be a chemical interaction (metabolic inhibition) as opposed to a physical interaction (membrane disruption, see Hugo & Denyer 1987; Denyer & Stewart 1998).

Hom (1972) explained the meaning of the dilution coefficient ( $n$ ), thus: the efficiency of disinfection decreases rapidly with dilution when the value of  $n$  is greater than one. The contact time is of greater importance than disinfectant concentration when the value  $n$  is less than one. For most chemical disinfectants, concentration and time are of equal importance when  $n$  is equal to one. In our study when using chlorite, the value of  $n$  was less than one (average  $n = 0.80$ ), which suggests that contact time is of greater importance than chlorite concentration.

The coefficient Q indicates the effectiveness of chlorite on AOB inhibition. The coefficient Q and pH value can be related by a linear fit as shown in Figure S-3. The equation

of this line is

$$Q = -0.0745 \text{ pH} + 0.768 \quad (4)$$

As pH increases,  $Q$  decreases. Note that the pH range applicable to this equation is between 7 and 9, the range normally found in distribution systems. Lower  $Q$  means a higher level of quenching (e.g., loss of disinfectant). It can be inferred that the ability of chlorite to inhibit AOB activity is reduced as the pH increases. As noted in Table 2,  $Q$  is equal to  $k_2 n$  for the IQ and equal to  $k_2 n^*$  for the mIQ model. Based on experimental results presented here, both rates  $k_1$  and  $k_2$  were governed by pH.

## SUMMARY AND CONCLUSION

This research introduces an innovative and alternative way to study nitrification inhibition. Instead of using the traditional method of quantifying cell concentration over time, the consumption of ammonia was measured. The term natural log reduction,  $\ln(A/A_0)$ , used in this paper refers to the reduction of ammonia concentration as a result of nitrification. The inhibition of *N. europaea* by chlorite can be modeled using the mIQ model that is first introduced in this study. This model is suitable for a natural log reduction-time curve with a high amount of tailing.

The modified IQ model describes the inhibition in which the natural log of activity is a function of three coefficients: the rate of AOB activity ( $k_1$ ), dilution coefficient ( $n^*$ ), and the amount of curvature ( $Q$ ) in plots. Coefficient  $Q$  is a product of  $k_2$  and  $n^*$ , where  $k_2$  is defined as the rate of chlorite effectiveness. Both  $k_1$  and  $Q$  coefficients were found to be dependent on pH in a range of 7 to 9. Other parameters such as ammonia concentration and temperature were shown to be less significant.

Water utilities are expected to benefit from this work as the measurements of ammonia loss and nitrite production are relatively fast and less costly compared to counting live and dead bacterial cells. Many water utilities do not have in-house capabilities for quantifying cell concentration. This alternative technique will significantly increase the validity of using chlorite as an inhibitor for controlling nitrification in the distribution system in its early state of

initiation. More work is needed to examine inhibition kinetics of chlorite on AOB growth in on-going or severe nitrification episodes. In order to minimize the impact of various external variables, we used water passing through a reverse osmosis membrane. In actual distribution system water, there can be interference from NOM. Therefore, future work should also cover the aspect of NOM effect in model development.

## ACKNOWLEDGEMENTS

The authors would like to acknowledge the East-West Center, who provided a graduate degree fellowship to the first author, and the Louisville Water Company for providing laboratory facilities and all other support. This is a contributed paper of the Water Resources Research Center, University of Hawaii.

## REFERENCES

- Agency for Toxic Substances and Disease Registry (ATSDR) 2004 *Toxicological Profile for Chlorine Dioxide and Chlorite*. US Department of Health and Human Services, Public Health Service, Atlanta, GA, <http://www.atsdr.cdc.gov/toxprofiles/tp.asp?id=582&tid=108>.
- Blute, N., Pedersen, D. W., Wu, X. & Means, E. 2013 Demonstration testing of nitrification control using chlorite in Irvine, Calif. *J. Am. Water Works Assoc.* **105** (4), E207–E216.
- Boulos, L., Prévost, M., Barbeau, B., Coallier, J. & Desjardins, R. 1999 LIVE/DEAD BacLight: application of a new rapid staining method for direct enumeration of viable and total bacteria in drinking water. *J. Microbiol. Methods* **37** (1), 77–86.
- Chick, H. 1908 An investigation into the laws of disinfection. *J. Hyg. (Lond.)* **8** (1), 92–158.
- Denyer, S. P. & Stewart, G. S. A. B. 1998 Mechanisms of action of disinfectants. *Int. Biodeterior. Biodegrad.* **41**, 261–268.
- Finch, G. R., Black, E. K., Labatiuk, C. W., Gyurek, L. & Belosevic, M. 1993a Comparison of *Giardia lamblia* and *Giardia muris* cyst inactivation by ozone. *Appl. Environ. Microbiol.* **59** (11), 3674–3680.
- Finch, G. R., Black, E. K., Labatiuk, C. W., Gyurek, L. & Belosevic, M. 1993b Ozone inactivation of *Cryptosporidium parvum* in demand-free phosphate buffer determined by in vitro excystation and animal infectivity. *Appl. Environ. Microbiol.* **59** (12), 4203–4210.

- Harms, G., Layton, A. C., Dionisi, H. M., Gregory, I. R., Garrett, V. M., Hawkins, S. A., Robinson, K. G. & Sayler, G. S. 2003 [Real-time PCR quantification of nitrifying bacteria in a municipal wastewater treatment plant](#). *Environ. Sci. Technol.* **37** (2), 343–351.
- Harrington, G. W., Noguera, D. R., Kandou, A. I. & Vanhoven, D. J. 2002 Pilot-scale evaluation of nitrification control strategies. *J. Am. Water Works Assoc.* **94** (11), 78–89.
- Hom, L. 1972 Kinetics of chlorine disinfection in an ecosystem. *J. Sanit. Eng. Div., Am. Soc. Civ. Eng.* **98** (1), 183–194.
- Hooper, A. B. 1989 Biochemistry of the nitrifying lithoautotrophic bacteria. In: *Autotrophic Bacteria* (H. G. Schlegel & B. Bowien, eds). Science and Technology Publishers, Madison, Wisconsin, pp. 239–265.
- Hugo, W. B. & Denyer, S. P. 1987 The concentration exponent of disinfectants and preservatives (biocides). In: *Preservatives in the Food, Pharmaceutical and Environmental Industries* (R. G. Board, M. C. Allwood & J. G. Banks, eds). The Society for Applied Bacteriology Technical Series 22, Blackwell Scientific Publications, Oxford, UK.
- Hynes, R. K. & Knowles, R. 1983 Inhibition of chemoautotrophic nitrification by sodium chlorate and sodium chlorite: a reexamination. *Appl. Environ. Microbiol.* **45** (4), 1178–1182.
- Lambert, R. J. W. & Johnston, M. D. 2000 [Disinfection kinetics: a new hypothesis and model of the tailing of log-survivor/time curves](#). *J. Appl. Microbiol.* **88** (5), 907–913.
- McGuire, M. J., Lieu, N. I. & Pearthree, M. S. 1999 Using chlorite ion to control nitrification. *J. Am. Water Works Assoc.* **91** (10), 52–61.
- McGuire, M. J., Pearthree, M. S., Blute, N. K., Arnold, K. F. & Hoogerwerf, T. 2006 Nitrification control by chlorite ion at pilot scale. *J. Am. Water Works Assoc.* **98** (1), 95–105.
- McGuire, M. J., Wu, X., Blute, N. K., Askenaizer, D. & Qin, G. 2009 Prevention of nitrification using chlorite ion: results of a demonstration project in Glendale, Calif. *J. Am. Water Works Assoc.* **110** (10), 47–59.
- O'Connor, T., Murphy, B. & O'Connor, J. T. 2001 Controlling nitrification in a water distribution system using sodium chlorite. *Water Eng. Manage.* **148** (9), 14–15.
- Odell, L. H., Kirmeyer, G. J., Wilczak, A., Jacangelo, J. G., Marcinko, J. P. & Wolfe, R. L. 1996 Controlling nitrification in chloraminated systems. *J. Am. Water Works Assoc.* **88** (7), 86–98.
- Oldenburg, P. S., Regan, J. M., Harrington, G. W. & Noguera, D. R. 2002 Kinetics of *Nitrosomonas europaea* inactivation by chloramine. *J. Am. Water Works Assoc.* **94** (10), 100–110.
- Passantino, L., Pressman, J., Chowdhury, Z., Devkota, L., Russell, J., Groendyk, A. & Swanson, W. 2003 Pipe-loop studies evaluating nitrification and disinfection by-product formation following the conversion to chloramines. In *Proceedings of the American Water Works Association's Annual Conference and Exposition*, Anaheim, California.
- Rungvetvuthivayata, M., Song, R., Campbell, M., Wang, J. & Ray, C. 2008 Development of chlorite CT equation for nitrification inhibition. In *Proceedings of the American Water Works Association's Annual Conference and Exposition*, Atlanta, GA.
- Skadsen, J. 2002 Effectiveness of high pH in controlling nitrification. *J. Am. Water Works Assoc.* **94** (7), 73–83.
- US Environmental Protection Agency (USEPA) 1989 Drinking water; national primary drinking water regulations; total coliforms (including fecal coliforms and *E. coli*); final rule. *Federal Register* **54** (124), 27543–27568.
- US Environmental Protection Agency (USEPA) 1997 *Method 300.1 Determination of Inorganic Anions in Drinking Water by Ion Chromatography, Revision 1.0*. National Exposure Research Laboratory, Office of Research and Development, Cincinnati, Ohio.
- US Environmental Protection Agency (USEPA) 2009 *National Primary Drinking Water Standards*. EPA 816-F-09-004, Office of Water (4606M), Washington, DC. <http://water.epa.gov/drink/contaminants/index.cfm#Primary>.
- Watson, H. E. 1908 [A note on the variation of the rate of disinfection with change in the concentration of the disinfectant](#). *J. Hyg. (Lond.)* **8** (4), 536–542.
- Wilczak, A., Jacangelo, J. G., Marcinko, J. P., Odell, L. H., Kirmeyer, G. J. & Wolfe, R. L. 1996 Occurrence of nitrification in chloraminated distribution systems. *J. Am. Water Works Assoc.* **88** (7), 74–85.
- Wolfe, R. L., Lieu, N. I., Izaguirre, G. & Means, E. G. 1990 Ammonia-oxidizing bacteria in a chlorinated distribution system: seasonal occurrence, distribution, and disinfection resistance. *Appl. Environ. Microbiol.* **56** (2), 451–462.
- Yang, J., Harrington, G. W. & Noguera, D. R. 2008 [Nitrification modeling in pilot-scale chloraminated drinking water distribution systems](#). *J. Environ. Eng.* **134** (9), 731–742.

First received 25 July 2013; accepted in revised form 8 January 2014. Available online 7 February 2014